

SUPPORTING INFORMATION

Hydrodeoxygenation of fatty acid esters catalyzed by Ni on nano-sized MFI type zeolites

Moritz W. Schreiber, Daniella Rodriguez-Niño, Oliver Y. Gutiérrez*, and Johannes A. Lercher*

*TU München, Department of Chemistry and Catalysis Research Center, Lichtenbergstrasse 4,
D-84747 Garching, Germany*

*Corresponding authors:

Oliver.Gutierrez@mytum.de

Tel. 0049 89 28912827, Fax 0049 89 28913544

Johannes.Lercher@ch.tum.de

Tel. 0049 89 28913540, Fax 0049 89 28913544

Table S1: Fatty acid composition in triglyceride mixture of microalgae oil

Fatty acid composition [wt%]												
C _{14:0}	C _{16:0}	C _{18:2}	C _{18:1}	C _{18:0}	C _{20:4}	C _{20:0}	C _{22:6}	C _{22:4}	C _{22:1}	C _{22:0}	C _{24:0}	Sterol
0.04	4.41	56.2	32.2	4.41	0.07	0.43	0.13	0.19	0.97	0.44	0.36	0.12

Nomenclature in lipid numbers: C_{x:y}:x number of carbon atoms in fatty acid chain; y number of double bonds in fatty acid chain

Crude microalgae oil was obtained from Verfahrenstechnik Schwedt GmbH.

Table S2. Diameter, dispersion, and concentration of accessible Ni atoms on different materials as determined from XRD, TEM, and hydrogen chemisorption.

Catalyst	XRD		
	Diameter [nm]	Dispersion [%]	Accessible Nickel atoms [μmol/g]
Ni/H-ZSM-5	10.5	9.6	157
Ni/Silicalite 1	10.0	10.1	174
Ni/n-H-ZSM-5	3.6	28.0	445
Ni/n-Silicalite 1	2.6	38.8	668
Catalyst	TEM		
	Diameter [nm]	Dispersion [%]	Accessible Nickel atoms [μmol/g]
Ni/H-ZSM-5	8.8	11.5	187
Ni/Silicalite 1	8.0	12.6	218
Ni/n-H-ZSM-5	2.3	43.7	693
Ni/n-Silicalite 1	2.4	41.9	721
Catalyst	Hydrogen chemisorption		
	Diameter [nm]	Dispersion [%]	Accessible Nickel atoms [μmol/g]
Ni/H-ZSM-5	12.9	7.9	128
Ni/Silicalite 1	8.4	12.0	207
Ni/n-H-ZSM-5	4.5	22.0	349
Ni/n-Silicalite 1	4.7	21.5	370

XRD: particle diameters were calculated based on deconvoluted XRD signals for the (111) plane reflection of Ni *via* the Scherrer equation (1), where τ is the particle size in Å, K is the shape factor (0.9 for spherical particles used), β is the line broadening at half the maximum intensity of the reflection $[2\theta]$ after subtraction of the instrumental line broadening (0.1 for used instrument), λ is the X-Ray wavelength of the used cathode and θ is the Bragg angle of the signal.

$$\tau = \frac{K \lambda}{\beta \cos \theta} \quad (1)$$

TEM: Particle diameters were calculated based on at least 300 particles obtained from at least 5 different areas of the catalyst on the carbon grid. The dispersion D based on the mean particle size was calculated following formula (2), with v_{Ni} being the volume occupied by a Ni atom (10.95 Å^3) and a_{Ni} is the surface area of Nickel atom (6.51 Å^2) and d_{VA} is the mean particle size. The concentration of accessible Ni atoms was calculated based on the amount of Ni on the catalyst per gram and the dispersion based on formula (3).

$$D = 6 \frac{(v_{Ni}/a_{Ni})}{d_{VA}} \quad (2)$$

$$c_{\text{accessible Ni atoms}} = D \frac{(m_{Ni}/M_{Ni})}{m_{\text{catalyst}}} \quad (3)$$

References

- 1 P.Scherrer, *Nachr. Ges. Wiss.*, 1918, **2**, 96.
- 2 G. Ertl, H. Knözinger, J. Weitkamp, *Handbook of Heterogeneous Catalysis*, 2008, **3**, Weinheim, Wiley VCH.

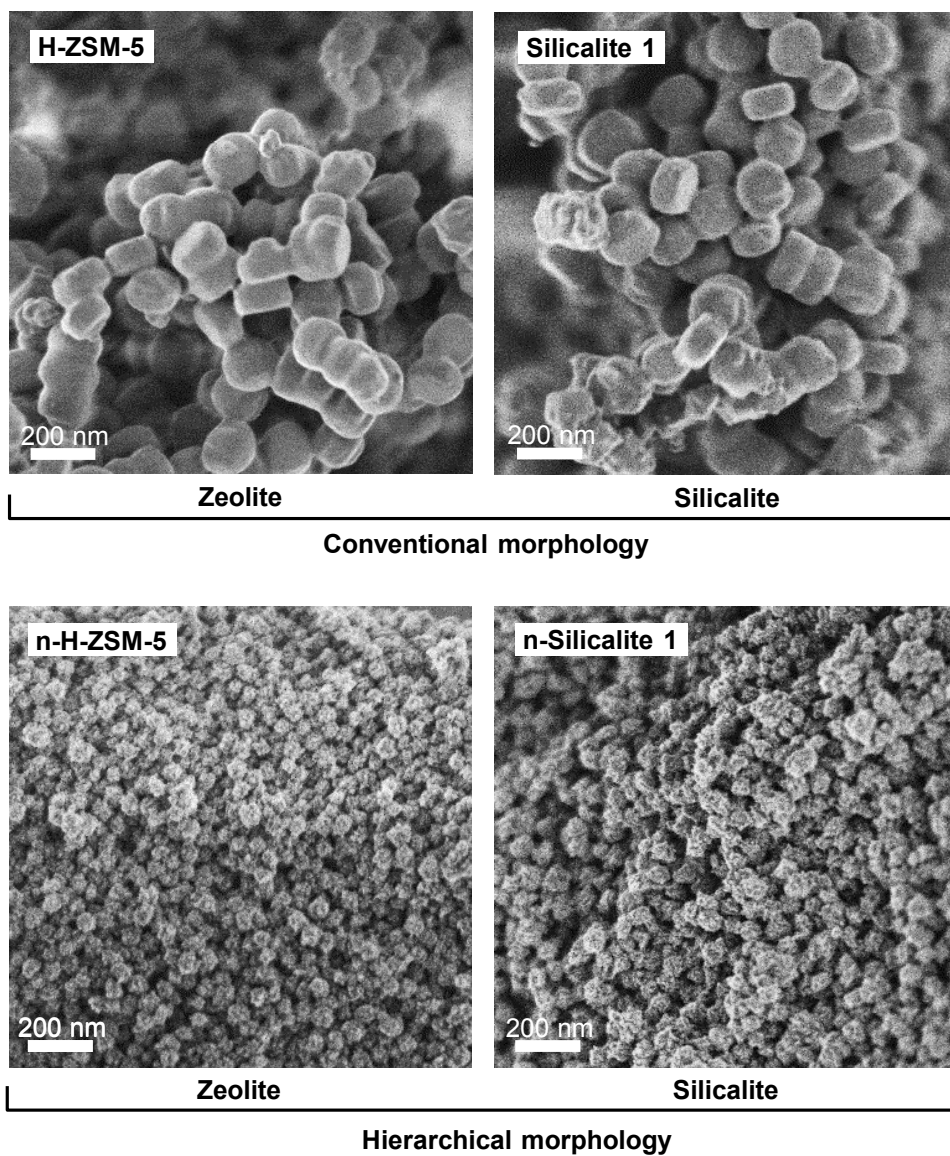


Figure S1. Representative micrographs of (n)-H-ZSM-5 and (n)-Silicalite 1 materials.

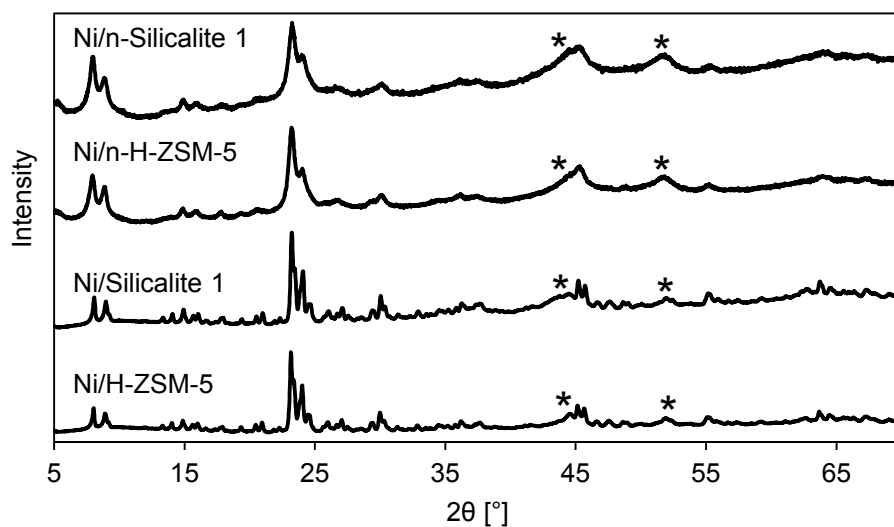


Figure S2. X-ray diffractograms of the catalysts based on (n)-H-ZSM-5 and (n)-Silicalite 1 materials. Nickel reflections are highlighted with a star (*).

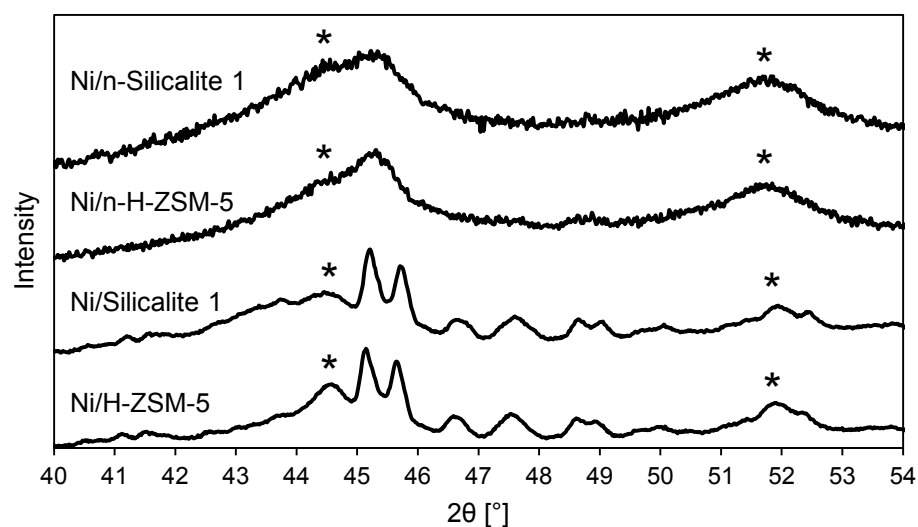


Figure S3. Detail of X-ray diffractograms in the region of Ni reflections of the catalysts based on (n)-H-ZSM-5 and (n)-Silicalite 1 materials). Nickel reflections are highlighted with a star (*).

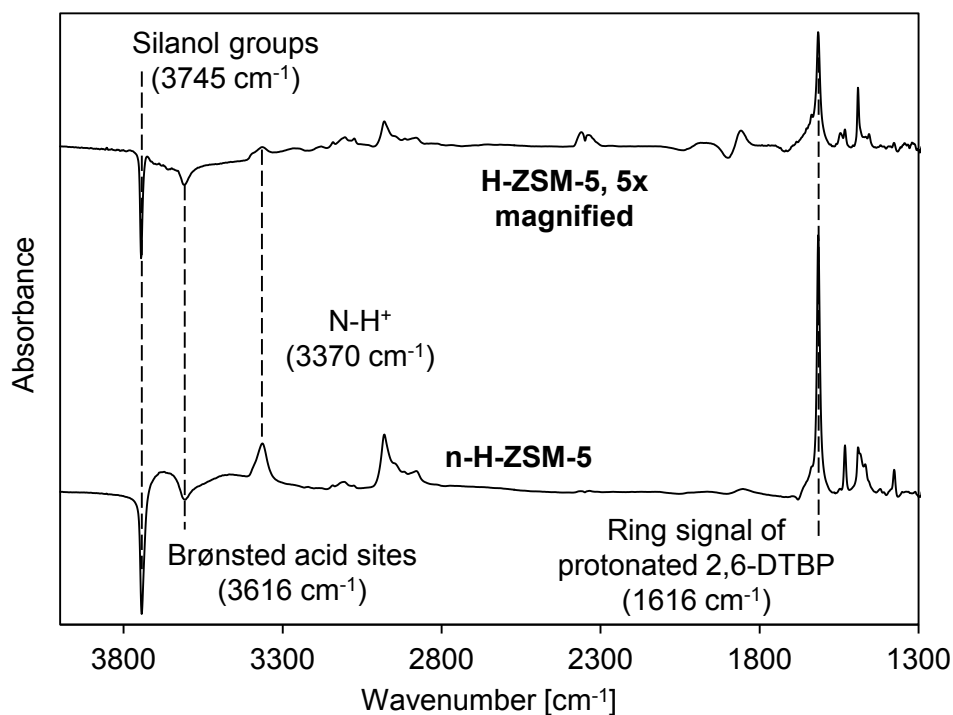


Figure S4. Changes in IR spectra after adsorption of 2,6-di-tert-butyl-pyridine (2,6-DTBP) at 423 K, 0.01 kPa and outgassing for 1 h in vacuum. The characteristic bands at 3370 cm^{-1} (N-H^+ vibration) and 1616 cm^{-1} ($\text{C}=\text{C}$ vibration) appear from 2,6-DTBP interaction with the zeolite.

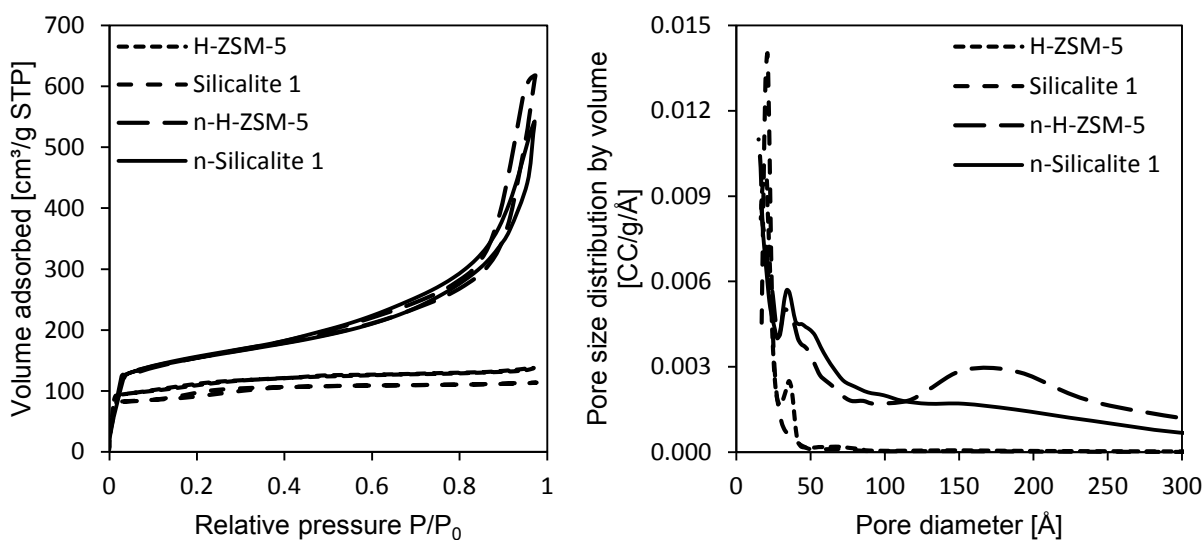


Figure S5. N_2 -physorption isotherms and pore size distributions of unloaded parent materials.

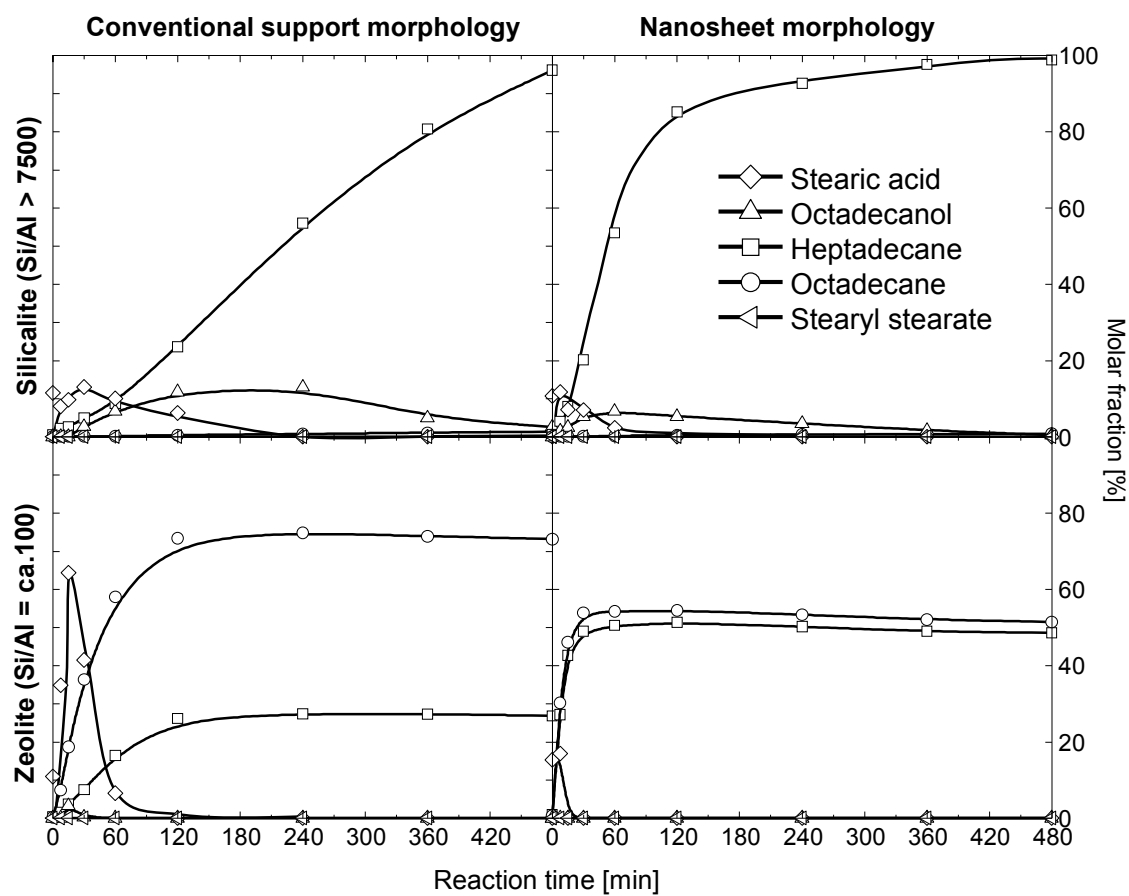


Figure S6. Evolution of the concentrations of reaction products of algae oil conversion over time.

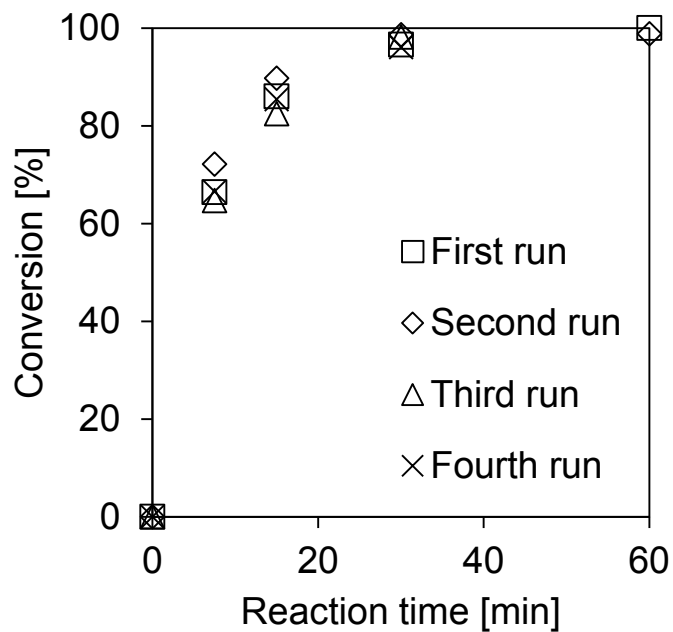


Figure S7. Evolution of algae oil conversion over time for four consecutive recycling experiments of Ni/n-H-ZSM-5.

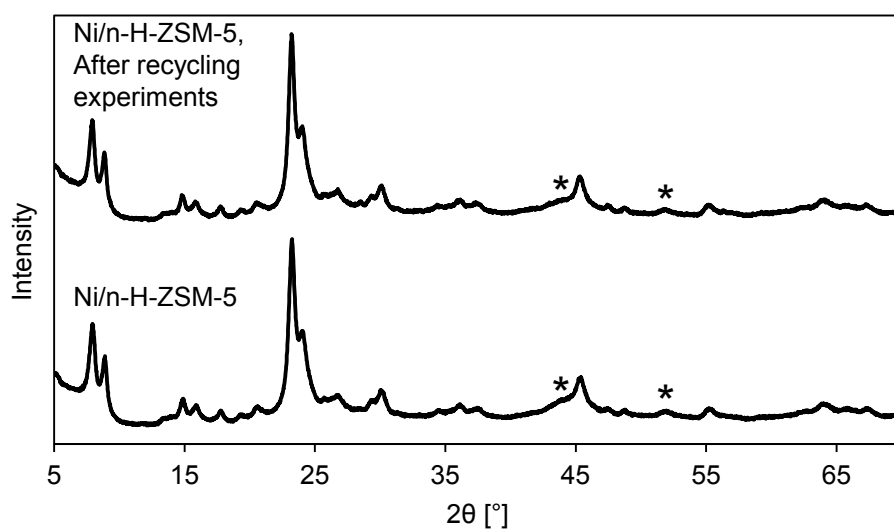


Figure S8. X-Ray diffractograms of Ni/n-H-ZSM-5 before and after four consecutive recycling experiments. Nickel reflections are labeled with “*”.

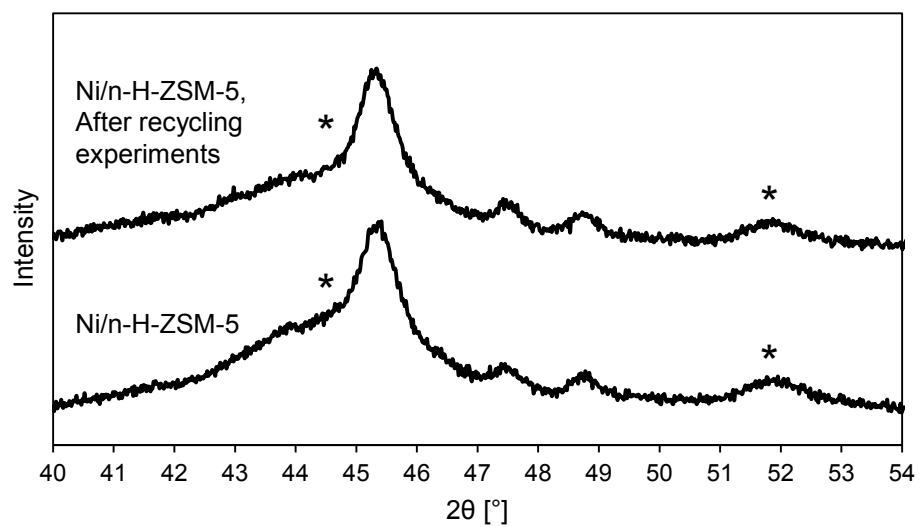


Figure S9. X-ray diffractograms of Ni/n-H-ZSM-5 before and after four consecutive recycling experiments. Nickel reflections are labeled with “*”.